Fuel Cells

DOI: 10.1002/anie.201001922

Catalytic Activity Enhancement for Oxygen Reduction on Epitaxial Perovskite Thin Films for Solid-Oxide Fuel Cells**

*Gerardo Jose la O', Sung-Jin Ahn, Ethan Crumlin, Yuki Orikasa, Michael D. Biegalski, Hans M. Christen, and Yang Shao-Horn**

Transition-metal oxides are commonly used as catalysts for the oxygen reduction reaction (ORR) in fuel cells for efficient power generation. The main barrier to achieving acceptable chemical-to-electrical conversion efficiency in fuel cells is the sluggish ORR kinetics at the cathode.[1] A lack of fundamental understanding of the ORR mechanism limits the development of highly active catalysts to enhance fuel cell efficiency. As single-crystal oxide thin films and superlattices can have physical properties dramatically different from those of bulk materials, such as enhanced ferroelectricity[2] and oxygen-ion conductivity,[3,4] one may expect that thin-film surfaces can have intrinsic ORR activity different from that of the bulk. However, studies to date have shown that polycrystalline[5,1b] and single-crystal epitaxial oxide films[6,7] have reduced ORR activity (specifically surface oxygen exchange kinetics) relative to the bulk (see Figure S1 in the Supporting Information). Herein, we report the epitaxial growth of a strontium-substituted lanthanum cobalt perovskite, $La_{0.8}Sr_{0.2}CoO_{3-\delta}$ (LSC), on (001)-oriented single-crystal yttria-stabilized zirconia. The epitaxial LSC surface exhibits markedly increased ORR activity by up to two orders of magnitude relative to the bulk, which may be attributed to increased oxygen vacancy concentrations in the films.

Pulsed laser deposition (PLD) was utilized to first deposit a gadolinium-doped ceria (GDC, 20 mol% Gd) film having a thickness of approximately 5 nm on a single crystal of yttria-stabilized zirconia (YSZ) with the $(001)_{cubic}$ orientation. LSC thin films with thicknesses of 20, 45, and 130 nm were subsequently deposited on the GDC/YSZ $(001)_{cubic}$ substrate. GDC was used as an interlayer to prevent chemical reactions between LSC and YSZ.[8] Atomic force microscopy (AFM) showed that LSC films had a surface root-mean-square (RMS) roughness of 3–6 nm (Figure 1a).

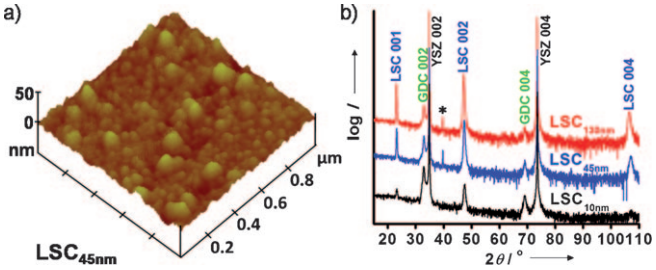

Figure 1. a) AFM image of an LSC_{45nm} film with surface RMS roughness of ca. 3.4 nm. b) Normal XRD data of LSC films of area 100 mm^2.

Normal X-ray diffraction (XRD) patterns (Figure 1b) of LSC thin films only reveal $(001)_{cubic}$ or $(00l)_{pc}$ peaks, which indicates $(001)_{pc}$LSC//$(001)_{cubic}$GDC//$(001)_{cubic}$YSZ. The subscript "pc" denotes the pseudocubic notation, in which the rhombohedral structure of LSC bulk[9] is approximated with $a_{pc} \approx 3.837$ Å (see Figure S2 in the Supporting Information). Four-circle XRD data analysis (see Figure S3 in the Supporting Information) showed that LSC films grown epitaxially on $(001)_{cubic}$YSZ were single-phase. In addition, off-normal XRD data (Figure 2a) showed that the $[100]_{pc}$LSC was rotated by 45° with respect to the $[100]_{cubic}$GDC, which is expected from $a(\text{GDC}) \approx \sqrt{2}a_{pc}(\text{LSC})$ (Figure 2b; that is, $[100]_{pc}$LSC//$[110]_{cubic}$GDC//$[110]_{cubic}$YSZ).

Of significance is the fact that the films have much larger relaxed unit cell volumes than the bulk[9] at room temperature. Having a different relaxed unit volume from that of bulk materials is commonly noted for PLD films, and may

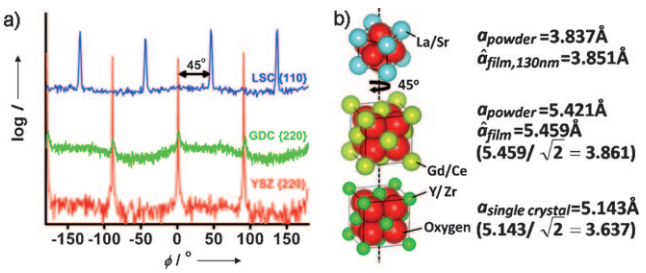

Figure 2. a) Off-normal XRD patterns of LSC_{130nm}//GDC//$(001)_{cubic}$YSZ. b) The cube-on-cube alignment of GDC on YSZ and the 45° in-plane rotation (ϕ) of LSC on GDC.

[*] Dr. G. J. la O',[+] Dr. S.-J. Ahn,[+] E. Crumlin, Y. Orikasa, Prof. Dr. Y. Shao-Horn
Electrochemical Energy Laboratory
Massachusetts Institute of Technology
Cambridge, MA 02139 (USA)
Fax: (+1) 617-258-7018
E-mail: shaohorn@mit.edu
Dr. M. D. Biegalski, Dr. H. M. Christen
Center for Nanophase Materials Sciences
Oak Ridge National Laboratory
Oak Ridge, TN 37831 (USA)
[+] These authors contributed equally to this work.

[**] This work was supported in part by the NSF (CBET 08-44526), DOE (SISGR DE-SC0002633), and King Abdullah University of Science and Technology. S.-J.A is grateful for financial support from the Korean Government (KRF-2008-357-D00119). The portion of research performed at ORNL CNMS was sponsored by the Scientific User Facilities Division, Office of Basic Energy Sciences, U.S. DOE.
Supporting information for this article is available on the WWW under http://dx.doi.org/10.1002/anie.201001922.

Table 1: Constrained and relaxed lattice parameters of LSC films extracted from normal and off-normal XRD data from 100 mm^2 samples. Constrained normal and in-plane lattice parameters of LSC films were calculated by combining the interplanar distance of the $(002)_{pc}$ and $(011)_{pc}$ peaks.

Materials	Constrained in-plane a [Å]	Constrained normal c [Å]	Relaxed film lattice parameter[a] $\hat{a}$ [Å]	In-plane strain $\varepsilon_{xx} = \frac{(a-\hat{a})}{\hat{a}}$ [%]	Normal strain $\varepsilon_{zz} = \frac{(c-\hat{a})}{\hat{a}}$ [%]
LSC_{20nm} (pc)	3.890	3.829	3.853	0.95	−0.63
LSC_{45nm} (pc)	3.915	3.825	3.861	1.40	−0.93
LSC_{130nm} (pc)	3.862	3.843	3.851	0.30	−0.20

[a] $\hat{a}$ was calculated from $\frac{\Delta c}{\hat{c}} = \frac{-2\nu}{1-\nu}\frac{\Delta a}{\hat{a}}$, assuming $\hat{a} = \hat{c}$ and $\nu = 0.25$[11] for LSC. [b] For LSC, $a_{pc} = (a_{rhom.}/2)\,(3-2\cos\alpha_{rhom.})^{1/2}$,[24] where $a_{rhom.} = 5.403$ and $\alpha_{rhom.} = 60.569°$.

result from a different oxygen nonstoichiometry[10,11] and/or microstructure.[6] LSC films were found to be dilated in-plane and compressed in the direction normal to the film surface at room temperature with good crystallinity (Table 1 and Figure S4 in the Supporting Information). The origin of these strains is not understood, but they might be a consequence of different thermal expansion coefficients between YSZ ($\approx 11\times10^{-6}\,°C^{-1}$)[12] and LSC films ($\approx 17\times10^{-6}\,°C^{-1}$ for bulk).[10] Experiments are ongoing to examine how these strains change upon heating to high temperatures.

The ORR activity of epitaxial LSC films was examined using electrochemical impedance spectroscopy (EIS) measurements conducted on patterned microelectrodes fabricated by photolithography and acid etching (see Figure S5 in the Supporting Information). EIS data collected from LSC films of thickness 20, 45, and 130 nm at 520 °C show similar features, and representative data of the 130 nm film measured as a function of are shown in Figure 3a. The real impedance (Z_{re}) of the predominant semicircle decreased significantly with increasing P_{O_2} (Figure 3a), which indicates that the surface oxygen exchange kinetics governs the ORR activity.[13] This is further supported by the fact that the film thicknesses are much smaller than the critical thickness (1 μm for LSC bulk[14]), above which oxygen diffusion limits ORR activity.

The electrical surface exchange coefficient, k^q, was extracted from the real impedance as a function of P_{O_2}. On the other hand, the chemical surface exchange coefficient, k_{chem}, which describes the rate of surface oxygen exchange with chemical driving force, can be deduced indirectly from the semicircle peak frequency, which is related to k^q by $k_{chem} = \gamma k^q$ (γ is the thermodynamic enhancement factor), as reported previously[13,15] (for details see the Supporting Information). In this deduction, it is assumed that the film surface has the same γ as the film bulk.[16] The P_{O_2} dependence ($k \propto P_{O_2}^m$) of k^q and k_{chem} was found to range from $m = 0.63$ to 0.89, as shown in Figure 3b. These values are in good agreement with those found for bulk LSC,[17] from which dissociative adsorption was proposed by Adler et al.[18] as rate-limiting for surface oxygen exchange.

The average, maximum, and minimum values of k^q and k_{chem} for each film thickness, obtained from measurements of multiple samples (see Figure S6 in the Supporting Information), are shown in Figure 3b. Remarkably, k^q and k_{chem} averages of the LSC films are higher than those extrapolated for LSC bulk[17,19] by about two orders of magnitude at 1 atm (Figure 3b). In addition, upon considering experimental

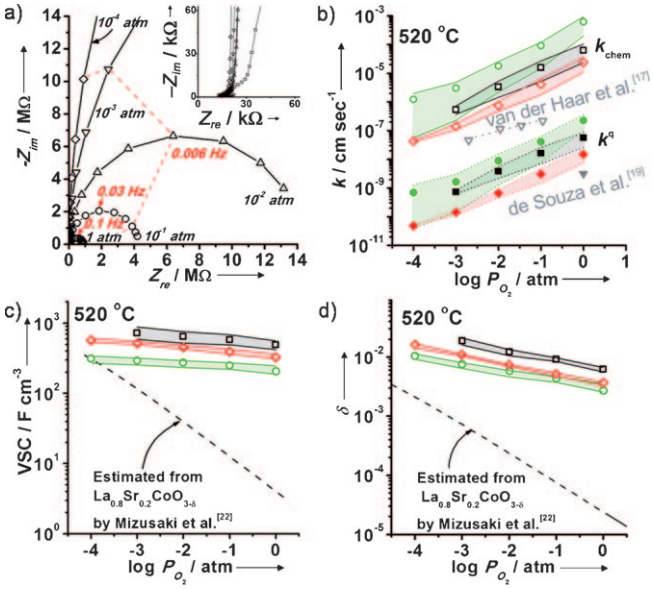

Figure 3. a) Typical EIS spectra of a LSC_{130nm} microelectrode with diameter 200 μm. Inset: the high-frequency intercept. b) k^q and k_{chem}, from LSC_{20nm} (green ○,●), LSC_{45nm} (□,■), and LSC_{130nm} (red ◇,◆) microelectrodes calculated from EIS spectra. Extrapolated k^* (approximately equivalent to k^q) and k_{chem} values obtained from previous studies of (▽) De Souza et al.[19] and (▼) van der Haar et al.[17] are plotted for comparison. c) VSCs of LSC_{20nm} (green ○), LSC_{45nm} (□), and LSC_{130nm} (red ◇) microelectrodes. d) Oxygen nonstoichiometry δ of LSC_{20nm}, LSC_{45nm}, and LSC_{130nm} films. Shaded areas mark the range of data scatter between maximum and minimum values from multiple samples as a function of P_{O_2}.

uncertainty, k^q and k_{chem} averages increase with decreasing film thickness at 1 atm but this trend becomes less apparent with decreasing P_{O_2}. Further studies are needed to reduce data scatter and verify the thickness-dependent k^q and k_{chem} values in Figure 3b. Moreover, higher surface oxygen exchange rates of LSC films relative to the bulk is in contrast to previous findings on epitaxial films of $PrBaCo_2O_{5+\delta}$ on $SrTiO_{3e}$ and $Nd_2NiO_{4+\delta}$ on YSZ,[7] which have k_{chem} and k^q values roughly two or three orders of magnitude lower than those of $PrBaCo_2O_{5+\delta}$[20] and $Nd_2NiO_{4+\delta}$[21] bulk, respectively.

The oxygen nonstoichiometry (δ) in the LSC films at 520 °C was estimated subsequently by using volume-specific capacitance (VSC) (see the Supporting Information). VSCs, indicative of changes in the oxygen nonstoichiometry induced

by changes in the electrical potential, were extracted from EIS data (see the Supporting Information). The average, maximum, and minimum values of each film are shown in Figure 3c, where the films have considerably larger VSCs than the bulk. Correspondingly, δ averages of LSC films are approximately 100 times greater than those of LSC bulk (extracted from the thermodynamic parameters of Mizusaki et al.[22]) at 1 atm, whereas they are about five times higher at 10^{-4} atm, as shown in Figure 3d. This is in contrast to the findings for micrometer-thick polycrystalline LSC films reported by Kawada et al.,[5] in which δ values estimated from EIS data of polycrystalline $La_{0.6}Sr_{0.4}CoO_{3-\delta}$ films at 600 °C are considerably lower than in the bulk,[22] with films having surface oxygen exchange coefficients reduced by as much as five times.

It is hypothesized that the enhanced k^q and k_{chem} of the LSC thin films may be attributed largely to higher oxygen nonstoichiometry in LSC films relative to the bulk. Although the 20-nm-thick film shows an oxygen nonstoichiometric value smaller than those of 45 and 130 nm films, the difference in δ among all the films is much smaller than that between films and the LSC bulk. While the physical origin of greater oxygen deficiencies in the epitaxial LSC films relative to the bulk is not clearly understood, the result in Figure 3d illustrates that these films may have a microstructure (including cation defects/vacancies and/or strains) different from that of the bulk, which can stabilize oxygen vacancies at high temperatures, as required for catalysts in the oxygen electrode.

Illustrating the importance of the film microstructure is the observation that LSC films have a larger relaxed unit cell volume than the bulk measured at room temperature. Presumably, these cation defects/vacancies and/or strains are more likely to occur near the epitaxial LSC/GDC interface, which may stabilize more oxygen vacancies as proposed in other epitaxial systems[3] and thus enhance surface oxygen exchange kinetics and ORR activity. This argument is supported by the fact that the k_{chem} values of epitaxial LSC films at $P_{O_2} \geq 0.1$ atm in this study are comparable to those estimated for the interfacial regions of $La_{0.6}Sr_{0.4}CoO_{3-\delta}/(La,Sr)_2CoO_{4+\delta}$ (8×10^{-6} cm s^{-1} at 0.2 atm and 500 °C).[23] Moreover, considering the uniaxial chemical expansion coefficient (chemical strain $= 0.037 \times \delta$) associated with oxygen nonstoichiometry changes of LSC reported previously,[10] very small uniaxial tensile strains of approximately 0.06 % would be sufficient to induce the difference in the δ value between the LSC films and bulk[22] shown in Figure 3d. Why epitaxial LSC/GDC/YSZ thin films in this study show enhanced surface exchange kinetics, while other epitaxial $Nd_2NiO_{4+\delta}$/YSZ and $PrBaCo_2O_{5+\delta}/SrTiO_3$ films have reduced values relative to the bulk materials, might be attributed to differences in the interfacial strains and defects, which will need to be clarified in future studies.

To our knowledge, this is the first report that epitaxial oxide films exhibit greatly enhanced surface oxygen exchange kinetics and ORR activity. The findings illustrate the potential to promote ORR activity on selected heterostructured oxide films, and provide new strategies to design highly active catalysts for applications in solid-oxide fuel cells, solid-oxide electrolytic cells, oxygen-conducting membranes, and high-temperature sensors.

Experimental Section

Single-crystal 9.5 mol % Y_2O_3-stabilized ZrO_2 (YSZ) wafers with (001) orientation and dimensions of $10 \times 10 \times 0.5$ mm (Princeton Scientific, USA) were used as substrate. Platinum ink (#6082, BASF, USA) counter electrodes were painted on one side of the YSZ and dried at 800 °C in air for 1 h. The PLD deposition of LSC with thicknesses of 20, 45, and 130 nm was performed by using a KrF excimer laser at $\lambda = 248$ nm, 10 Hz pulse rate, and 50 mJ pulse energy under P_{O_2} of 10 mTorr at 680 °C. After deposition, the sample was cooled to room temperature in ≈ 1 h under a P_{O_2} of 0.013 atm. Elemental analysis of representative LSC films by Rutherford backscattering spectroscopy revealed an average film composition of (15.0 ± 0.5) at.% La, (3.5 ± 0.5) at.% Sr, (17.5 ± 1.0) at.% Co, and (64.0 ± 5.0) at.% O, which is very close to the nominal stoichiometry of LSC.

Thin-film XRD was performed with a four-circle diffractometer (Bruker D8, Germany). Measurements were performed in normal and off-normal configurations. The LSC microelectrode patterns were fabricated by means of photolithography and chemical etching.[25] Microelectrode geometry and morphology were examined by optical microscopy (Carl Zeiss, Germany) and AFM (Veeco, USA).

The LSC microelectrode and porous Pt counter electrode were contacted by Pt-coated tungsten probes (see Figure S3 in the Supporting Information). EIS measurements of microelectrodes ≈ 200 μm in diameter were performed with three samples of 20 and 45 nm films, and two samples of 130 nm films by using a microprobe station (Karl Süss, Germany) connected to a frequency response analyzer (Solartron 1260, USA) and dielectric interface (Solartron 1296, USA). The temperature was controlled at 520 °C with a heating stage (Linkam TS1500, UK) and data were collected between 1 MHz and 1 mHz using a voltage amplitude of 10 mV. EIS experiments were completed under Ar and O_2 mixtures in the P_{O_2} range of 10^{-4} to 1 atm. Details of EIS data analysis can be found in the Supporting Information.

Received: March 31, 2010
Revised: May 4, 2010
Published online: June 22, 2010

Keywords: electrochemistry · epitaxy · fuel cells · heterogeneous catalysis · perovskite phases

[1] a) B. C. H. Steele, A. Heinzel, *Nature* **2001**, *414*, 345; b) S. B. Adler, *Chem. Rev.* **2004**, *104*, 4791; c) N. Q. Minh, *J. Am. Ceram. Soc.* **1993**, *76*, 563; d) H. A. Gasteiger, S. S. Kocha, B. Sompalli, F. T. Wagner, *Appl. Catal. B* **2005**, *56*, 9.

[2] J. Wang, J. B. Neaton, H. Zheng, V. Nagarajan, S. B. Ogale, B. Liu, D. Viehland, V. Vaithyanathan, D. G. Schlom, U. V. Waghmare, N. A. Spaldin, K. M. Rabe, M. Wuttig, R. Ramesh, *Science* **2003**, *299*, 1719.

[3] J. Garcia-Barriocanal, A. Rivera-Calzada, M. Varela, Z. Sefrioui, E. Iborra, C. Leon, S. J. Pennycook, J. Santamaria, *Science* **2008**, *321*, 676.

[4] a) X. Guo, *Science* **2009**, *324*, 2; b) N. Schichtel, C. Korte, D. Hesse, J. Janek, *Phys. Chem. Chem. Phys.* **2009**, *11*, 3043.

[5] T. Kawada, J. Suzuki, M. Sase, A. Kaimai, K. Yashiro, Y. Nigara, J. Mizusaki, K. Kawamura, H. Yugami, *J. Electrochem. Soc.* **2002**, *149*, E252.

[6] G. Kim, S. Wang, A. J. Jacobson, Z. Yuan, W. Donner, C. L. Chen, L. Reimus, P. Brodersen, C. A. Mims, *Appl. Phys. Lett.* **2006**, *88*, 3.

[7] A. Yamada, Y. Suzuki, K. Saka, M. Uehara, D. Mori, R. Kanno, T. Kiguchi, F. Mauvy, J. C. Grenier, *Adv. Mater.* **2008**, *20*, 4124.
[8] a) T. Tsai, S. A. Barnett, *Solid State Ionics* **1997**, *98*, 191; b) A. Tsoga, A. Gupta, A. Naoumidis, P. Nikolopoulos, *Acta Mater.* **1999**, *48*, 4709; c) J. M. Ralph, A. C. Schoeler, M. Krumpelt, *J. Mater. Sci.* **2001**, *36*, 1161; d) M. Shiono, K. Kobayashi, T. L. Nguyen, K. Hosoda, T. Kato, K. Ota, M. Dokiya, *Solid State Ionics* **2004**, *170*, 1.
[9] R. H. E. van Doorn, A. J. Burggraaf, *Solid State Ionics* **2000**, *128*, 65.
[10] X. Y. Chen, J. S. Yu, S. B. Adler, *Chem. Mater.* **2005**, *17*, 4537.
[11] H. M. Christen, E. D. Specht, S. S. Silliman, K. S. Harshavardhan, *Phys. Rev. B* **2003**, *68*, 020101.
[12] T. Ishihara, T. Kudo, H. Matsuda, Y. Takita, *J. Electrochem. Soc.* **1995**, *142*, 1519.
[13] S. B. Adler, J. A. Lane, B. C. H. Steele, *J. Electrochem. Soc.* **1996**, *143*, 3554.
[14] R. A. De Souza, J. A. Kilner, *Solid State Ionics* **1999**, *126*, 153.
[15] a) S. Wang, J. Yoon, G. Kim, D. Huang, H. Wang, A. J. Jacobson, *Chem. Mater.* **2010**, *22*, 776; b) S. B. Adler, *Solid State Ionics* **1998**, *111*, 125.
[16] J. Maier, *Solid State Ionics* **1998**, *112*, 197.
[17] L. M. van der Haar, M. W. den Otter, M. Morskate, H. J. M. Bouwmeester, H. Verweij, *J. Electrochem. Soc.* **2002**, *149*, J41.
[18] S. B. Adler, X. Y. Chen, J. R. Wilson, *J. Catal.* **2007**, *245*, 91.
[19] R. A. De Souza, J. A. Kilner, *Solid State Ionics* **1998**, *106*, 175.
[20] G. Kim, S. Wang, A. J. Jacobson, L. Reimus, P. Brodersen, C. A. Mims, *J. Mater. Chem.* **2007**, *17*, 2500.
[21] E. Boehm, J. M. Bassat, P. Dordor, F. Mauvy, J. C. Grenier, P. Stevens, *Solid State Ionics* **2005**, *176*, 2717.
[22] J. Mizusaki, Y. Mima, S. Yamauchi, K. Fueki, H. Tagawa, *J. Solid State Chem.* **1989**, *80*, 102.
[23] M. Sase, K. Yashiro, K. Sato, J. Mizusaki, T. Kawada, N. Sakai, K. Yamaji, T. Horita, H. Yokokawa, *Solid State Ionics* **2008**, *178*, 1843.
[24] D. Fuchs, L. Dieterle, E. Arac, R. Eder, P. Adelmann, V. Eyert, T. Kopp, R. Schneider, D. Gerthsen, H. von Lohneysen, *Phys. Rev. B* **2009**, *79*, 024424.
[25] G. J. la O', R. F. Savinell, Y. Shao-Horn, *J. Electrochem. Soc.* **2009**, *156*, B771; G. J. la O', B. Yildiz, S. McEuen, Y. Shao-Horn, *J. Electrochem. Soc.* **2007**, *154*, B427.

